Article

Separation of Monosaccharide Anomers on Photo-Click Cysteine-Based Stationary Phase: The α/β Interconversion Process Studied by Dynamic Hydrophilic Liquid Chromatography

Andrea Calcaterra [1], Simone Manetto [1,*], Fabio Buonsenso [1], Antonio Francioso [2,3], Marco Pierini [1] and Claudio Villani [1,*]

[1] Department of Chemistry and Drug Technology, Sapienza University of Rome, 00185 Rome, Italy
[2] Department of Biological Chemistry, Sapienza University of Rome, 00185 Rome, Italy
[3] Department of Organic Chemistry, Instituto Universitario de Bio-Organica "Antonio González", University of La Laguna, 38206 La Laguna, Spain
[*] Correspondence: simone.manetto@uniroma1.it (S.M.); claudio.villani@uniroma1.it (C.V.)

Abstract: In High-Performance Liquid Chromatography (HPLC), the separation of reducing sugars can typically show three possible typologies of chromatographic profiles (i.e., single peak, two resolved peaks and two peaks interconnected by a plateau) due to the rate at which the relevant α/β anomers interconversion (anomerization) can take place in relation to their elution-time. By analyzing these chromatographic profiles, thermodynamic and kinetic properties of anomerization phenomenon can be extrapolated. In this work we studied the anomerization of some monosaccharides by using a recently developed photo-click cysteine-based stationary phase through dynamic hydrophilic interaction liquid chromatography (D-HILIC) conditions. In the 5–25 °C temperature range, the $\Delta G^{\#}_{\alpha \to \beta}$ and $\Delta G^{\#}_{\beta \to \alpha}$ barriers were found to achieve values within the interval 21.1/22.2 kcal/mol for glucose, with differences between α→β and β→α reactions of about 0.4 kcal/mol. For xylose, in the same temperature range, the $\Delta G^{\#}_{\alpha \to \beta}$ and $\Delta G^{\#}_{\beta \to \alpha}$ barriers are between 20.7 to 21.5 kcal/mol, with differences between α→β and β→α reactions of about 0.2 kcal/mol. The experimental data are in agreement with those reported in literature, confirming the this new stationary phase using HILIC conditions is a robust platform to measure kinetic and thermodynamic properties of the isomerization reaction.

Keywords: monosaccharide anomers; D-HILIC; D-HPLC; interconversion energy barrier; Auto-DHPLC-Y2K; DCXplorer

1. Introduction

Carbohydrates (i.e., mono-, disaccharides and oligosaccharides) play an essential role in many vital processes, being at the basis of the metabolism of all living organisms. Compounds so widespread influence many scientific and industrial fields, e.g., biology, medicine, and the food industry, where it becomes essential to tackle their chemical characterization [1–3]. In particular, looking at the carbohydrates investigation through the chromatographic techniques, it is well known their separation faces three main critical issues: (i) they are very polar compounds; (ii) they are free of chromophores [4,5]; (iii) their structural complexity, characterized by the presence of different isomers, such as anomers (namely, in solution, reducing sugars exist in a mutarotation equilibrium between α- and β-anomers) [6].

High-Performance Liquid Chromatography (HPLC) represents the most used analytical methodology for analysing monosaccharide constituents of polysaccharides due to the high selectivity, sensitivity and versatility [7]. It allows detecting the presence of neutral, acidic and basic sugars through the wide range of stationary phases that have been

developed in recent years, combined with an adequate choice of the mobile phase and detectors to be used [8].

Regarding the first critical point in sugar chromatographic analysis, considering the most common elution mode, namely the reversed-phase HPLC (RP-HPLC), these analytes are not retained due to their high polarity, therefore alternative analysis techniques have been developed, such as the use of Hydrophilic Interaction Liquid Chromatography (HILIC). HILIC is based on the use of stationary phases consisting of strongly hydrophilic polar adsorbent substances in highly organic mixed mobile phases (mixtures of water or buffer (<40%) with organic solvents) [9–12]. This type of elution mode can provide excellent performance in separating monosaccharides [13]. The HILIC stationary phases most cited in the literature for the sugar analysis are the amino [7,9,14–16] and the amide [1,9,13,17,18] bonded stationary phases. Diol [5], cyclodextrin [9], and sugar-derivatized silica gel [19] also deserve to be mentioned.

About the second point, due to the absence of chromophores for the direct analysis of sugars, it is necessary to choose detectors other than UV-VIS ones. Compared to the well-known refractive index detector (RID), the Evaporative Light Scattering Detector (ELSD) shows higher sensitivity and higher chromatographic baseline stability. Other detectors that can be used for this purpose are the Charged Aerosol Detector (CAD) and Mass Spectrometry (MS) [4,20]. To be mentioned, in addition, the Pulsed Amperometric (PAD), and fluorescence detector [10,21–24].

Finally, regarding the structural complexity of monosaccharides, in HPLC analysis, anomers are considered somewhat of an analytical annoyance and to be avoided, as they produce at least band broadening, or even peak splitting into many separation systems. The most common way to minimize this problem is to raise the column temperature to render the anomer interconversion faster than chromatographic separation, it might be suitable to work in gradient conditions [25]. Moreover, some mobile phases and stationary phases are less discriminating toward anomers. However, HPLC can be used as a tool for studying the interconversion phenomena such as the one of sugar anomers. Two strategies can be used: (i) when interconversion $t_{1/2}$ > retention time, multiple injections from the same vial to evaluate the kinetics of interconversion are performed [4]; (ii) when interconversion $t_{1/2} \approx$ retention time, the study of the mutarotation phenomenon can be carried out by analyzing the profile of the characteristic dynamic chromatogram observed [17,25]. In this scenario, the retention of monosaccharides and disaccharides was investigated using a photo-click cysteine-based stationary phase recently introduced by some authors of this work. The zwitterionic structure of the phase prompted us to enlarge the potential of applicability in the HILIC mode and sugars are suitable compounds to be analyzed. Interestingly, after investigating different mono-, disaccharides and polyols, we observed the typical plateau between the two peaks confirming the presence of interconversion process for some monosaccharides. In detail, the anomers interconversion of the D-glucose and D-xylose sugars through the dynamic chromatography technique in HILIC conditions, was studied. The dynamic chromatograms obtained at different temperatures were processed using two computational software, Auto-DHPL-Y2K and DCXplorer, to extrapolate the related kinetic and thermodynamic data (i.e., $\Delta G^{\#}$, $\Delta H^{\#}$ and $\Delta S^{\#}$ and k_{app}) [25–29].

2. Experimental Section

2.1. Materials and Methods

2.1.1. Materials

Spherical Kromasil Si 100 silica gel (pore size 100Å, particle size 5.0 μm, specific surface area 340 m^2/g) was purchased from Akzo Nobel (Bohus, Sweden).

Vinyl triacetoxysilane, L-cysteine, potassium bromide FTIR grade (KBr), ammonium acetate, deuterium oxide (D$_2$O), acetonitrile d-3 (CD$_3$-CN), acetonitrile (ACN), methanol (MeOH), water HPLC grade and dry toluene were purchased from Sigma Aldrich (St. Louis, MO, USA), as well as the compounds used as standard (naphthalene, uracil,

adenine, cytosine, fructose, ribose, sucrose, maltose, lactose, lactulose, mannitol, inositol, D-glucose, D-xylose).

2.1.2. Instruments

The chromatographic runs were performed on a high-performance liquid chromatograph Waters, equipped with a 2487 dual wavelength absorbance detector (Waters, Milford, MA, USA) in series with a SEDEX 55 ELSD (S.E.D.E.R.E, France), 1525 binary HPLC pump and Rheodyne Model 7725i 20 μL loop manual injector (Rheodyne, Cotati, CA, USA). The elemental analysis was carried out using an elemental analyzer EA 1100 (Carlo Erba, Milan, Italy). Chromatographic data were collected and processed using Empower software, version 2.0. Simulations of variable temperature experimental chromatograms presenting a dynamic profile were performed with Auto-DHPLC-y2k (Auto-Dynamic-HPLC) written by Professor Marco Pierini (Sapienza University of Rome, Rome, Italy), and DCXplorer version 3.1.0.1, written by Professor Oliver Trapp (Ludwig-Maximilians-University, LMU, Munich, Germany). The two software are based on the classic stochastic mathematical model. A simplex algorithm can automatically optimize chromatographic and kinetic parameters until the best agreement between experimental and simulated dynamic chromatograms is achieved.

2.1.3. Columns

The photo-click cysteine-based stationary phase (VSG_HD-1-Photo-Cys) was prepared as some authors of this work recently reported [30]. Using the photo-click procedure described, it is possible to significantly increase the bond of cysteine on the silica surface, as shown by the data relating to the loading of the selector obtained from the elemental analysis. The loading of the selector of VSG_HD-1-Photo-Cys is 3.79 μmol/m^2 (1.35 mmol/g silica), much higher than that obtained by Shen et al. using a procedure that involves the use of a radical initiator (azoisobutyronitrile, AIBN), in this second case the loading was 1.52 μmol/m^2 [31].

Stainless steel columns (150 mm × 4.6 mm L × I.D.) supplied by Alltech Supply Inc (Woodridge, IL, USA) were packed with developed stationary phases VSG_HD-1-Photo-Cys and used in this work.

Other in-house made columns (150 × 4.1 mm L × I.D.) were used for comparison: USP-HILIC-NH2-sil, APS-2-Hypersyl and Click Lactose Hydrophobic [19].

2.1.4. Sample Preparation

(a)   Standard solution preparation

The HILIC test solution was a mixture of naphthalene, uracil, adenosine, and cytosine, solved in the mobile phase, at the concentration of 1 mg/mL each. The sugar solutions shown in Table 1 were prepared by dissolving a single sugar in the relative mobile phase at a final concentration of 1 mg/mL, the composition of the mobile phase was 80/20 ACN/H$_2$O (% *v/v*).

Table 1. Chromatographic data of sugars' separation performed on the VSG_HD-1-Photo-Cys.

Classification	Analyte	T (°C)	Ret. Time (min)	Mobile Phases
Monosaccharide	Fructose	25	8.66	ACN/H$_2$O 80:20
	Ribose	25	5.01	ACN/H$_2$O 80:20
Disaccharide	Sucrose	25	3.62	ACN/H$_2$O 60:40
	Maltose	25	4.00	ACN/H$_2$O 60:40
	Lactose	25	4.04	ACN/H$_2$O 60:40
	Lactulose	25	3.92	ACN/H$_2$O 60:40
Sugar Alcohol	Mannitol	25	11.22	ACN/H$_2$O 80:20
	Inositol	25	4.56	ACN/H$_2$O 60:40

(b)   Determination of the ratio between the two α/β anomers in equilibrium by ^{1}H-NMR

According to the non-linear response of the ELSD detector [32], the determination of the relative quantities of the two anomeric species α and β in solution at equilibrium, both for D-glucose and D-xylose, is required for the calculation of the K_{eq}. In order to extrapolate the kinetic parameters of the anomerization process, the determination of the ratio between the two α/β anomers in equilibrium was carried out by ^{1}H-NMR spectroscopic analysis of equilibrated solutions (25 °C; 72 h) of the two sugars at a known concentration (2 mg/mL) in CD_3CN/D_2O 85/15 (% *v/v*). The monosaccharide samples used for the chromatographic analyses were prepared by dissolving the compound in a mixture of ACN/H_2O 85/15 (% *v/v*) at a final concentration of 1 mg/mL and analysed after 72 h from the preparation to be sure that the equilibrium was achieved.

3. Results and Discussion

3.1. Stationary Phase and HILIC Performances

The stationary phase involved in this study, VSG_HD-1-Photo-Cys, was based on cysteine as selector which has been bonded on the high-density vinyl silica through a photo click reaction. The horizontal polymerization of vinyl units on the surface together with the photo-induced approach provided a final stationary phase extremely passivated with high loading of selector [30]. This approach renders the secondary non-specific interactions (due to the residual unreacted surface silanols) practically negligible, enhancing, thus, the polarity of the zwitterionic selector alone. The chromatographic performances of VSG_HD-1-Photo-Cys in HILIC mode were carried out by eluting a mixture consisting of four analytes with increasing polarity and the results were compared with three HILIC stationary phases: USP-HILIC-NH2-sil, APS-2-Hypersyl and Click Lactose Hydrophobic.

The elution order of the analytes on the stationary phases taken into consideration is naphthalene, uracil, adenosine and cytosine. By inspection of recorded chromatograms (Figure 1), the VSG_HD-1-Photo-Cys column shows a higher selectivity than others, especially between peaks 3 and 4 (i.e., adenosine and cytosine) bearing a sugar fragment in their structure. Its performance results comparable to that obtained on "click lactose hydrophobic" stationary phase, previously developed in our lab. In addition, the good peak symmetry confirms the slight contribution of residual silanols.
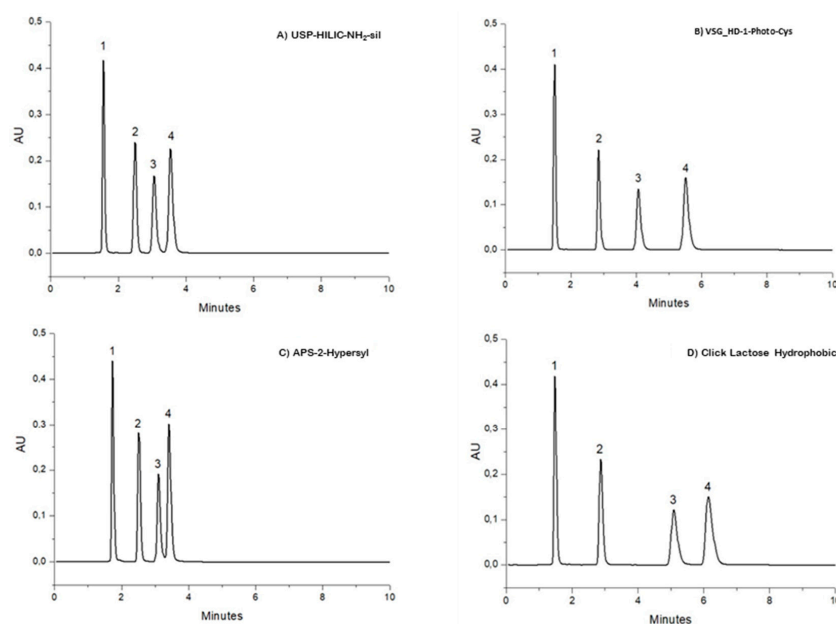
Figure 1. Chromatograms (HILIC test) carried out by eluting a mixture consisting of (**1**) naphthalene, (**2**) uracil, (**3**) adenosine and (**4**) cytosine (as in elution order) performed on the (**A**) USP-HILIC-NH2-sil, (**B**) VSG_HD-1-Photo-Cys, (**C**) APS-2-Hypersyl and (**D**) Click Lactose Hydrophobic stationary phases. Mobile phase: 80/20 ACN/H_2O (% *v/v*), flow rates: (**B**) 1 mL/min, and (**A,C,D**) 0.8 mL/min. Column temperature: 25 °C; injection volume: 5 μL, Chromatograms were recorded at 254 nm.

3.2. Sugar Retention

To investigate the potential of the HILIC method developed using the VSG_HD-1-Photo-Cys column for application in carbohydrates separation, two monosaccharides (fructose and ribose), four disaccharides (sucrose, maltose, lactose, and lactulose) and two sugar alcohol (mannitol and inositol) were selected. The results of the analyses and the experimental conditions are presented in Table 1. A good selectivity is observed, especially in the separation of monosaccharides and sugar alcohols (Chromatograms are reported in Supplementary Material Figure S1).

3.3. Dynamic HPLC Experiments: A Brief Overview

The tendency to isomerize of compounds endowed with structures containing labile stereogenic elements (such as centers, and axes) is commonly addressed by performing on these species kinetic studies able to provide the rate constants (k_v) for the forward (a→b) and backward (a←b) reactions of the process. Afterwards, starting from these data, the relevant activation free energy barriers ($\Delta G^{\#}_{a \to b}$ and $\Delta G^{\#}_{a \leftarrow b}$) can also be obtained by using the Eyring equation, together with the related enthalpic and entropic contributions (i.e., $\Delta H^{\#}$ and $\Delta S^{\#}$), obtained from the slope and the intercept of $\Delta G^{\#}/T$ vs. $1/T$ plots, when the kinetic study is carried out at different temperatures. Kinetic data are frequently obtained by resorting to either spectroscopic (e.g., UV, HNMR) or chromatographic (off-column batch-wise approach) quantitative analysis repeated over time on the isomerizing sample, kept at a defined and constant temperature. Two further methods, again based on chromatographic technique and employable to effectively perform the above mentioned kinetic studies, are known with the terms of "stopped-flow HPLC technique" and "dynamic chromatography". Dynamic chromatography (D-HPLC) makes possible to carry out fast and accurate k_v determinations of isomerization processes characterized by $\Delta G^{\#}$ values included within an extensive range, from about 15 kcal/mol to 38 kcal/mol, we have chosen this approach to perform the kinetic study reported herein. The principle on which D-HPLC is based, requires that the dynamic equilibrium of isomerization to be investigated takes place during a classical chromatographic run, to the outcome is an elution profile in which the peaks of the distinct isomers are separated by a "high baseline", that is, a "plateau zone" (a profile named "dynamic chromatogram"). The shape and height of the plateau are necessary to accurately estimate the forward and backward kinetic constants k_v (i.e., $k_v^{a \to b}$ and $k_v^{b \to a}$) leading the process. Simulations of such profiles with dedicated computer programs will provide the searched $k_v^{a \to b}$ and $k_v^{b \to a}$ values. In general, it is possible to distinguish between three main morphologies of chromatograms involving a mixture of species susceptible to isomerization (Figure 2), which are strongly dependent on the residence time and on the selected temperature:

(a) The dynamic profile of case I is associated with experimental conditions in which all molecules of both species A and B have undergone at least one cycle of interconversion during their discrimination inside the chromatographic column. As a result, a single peak of A and B in the mixture is eluted, characterized by a retention time intermediate between those of the single isomers. This dynamic chromatogram is not suitable for obtaining kinetic information.

(b) The dynamic profile reported in case II refers to a good chromatographic resolution of isomers A and B concomitant with an active, although only partial, interconversion between the same species during the discrimination process. In practice, only a fraction of the injected molecules underwent interconversion during the separation process. This dynamic chromatogram is the only one suitable for obtaining kinetic information by comparison with computational simulation.

(c) Profile of case III is obtained if, during the chromatographic run, the injected isomers A and B are effectively discriminated in two well baseline-separated peaks, without any concomitant, interconversion process occurred during the run. This kind of chromatograms could be employed in off-column batch-wise determinations but, obviously, not in DC measurements.
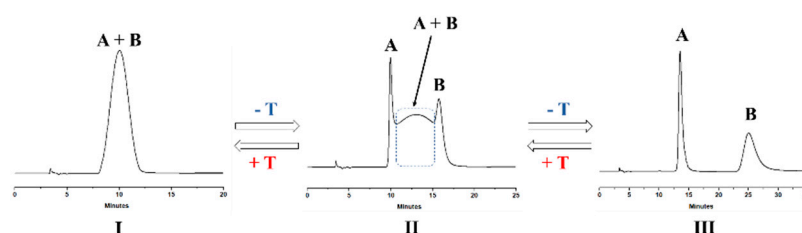
Figure 2. Typical profiles of dynamic chromatograms related to chromatographic resolution of species A and B which undergoes interconversion (cases I and II) or not (case III) during their HPLC discrimination (dependence of plateau zone on different rates of interconversion).

Computational simulations of dynamic chromatograms usually are based on two typologies of mathematical models: the Theoretical Plate Model and the Classic Stochastic Model. Both are implemented into the Auto-DHPLC-Y2K software [27], while only the second one within the computer program DCXplorer [28,29]. These two softwares have been used for the simulations performed in the present work, and the obtained results compared one to each other (Tables 2 and 3), confirming their reliability and their effectiveness.

Table 2. Values of $\Delta G^{\#}$ and kv_{app} for the processes that lead from the α to the β anomer of D-Glucose, and vice-versa, obtained by simulating experimental dynamic chromatograms with the Auto-DHPLC-Y2K and DCXplorer programs.

	D-Glucose							
	$\alpha \to \beta$				**$\beta \to \alpha$**			
	$\Delta G^{\#}{}_{\alpha \to \beta}$ (kcal mol^{-1})		**$kv_{app}{}^{\alpha \to \beta}$ (min^{-1})**		**$\Delta G^{\#}{}_{\beta \to \alpha}$ (kcal mol^{-1})**		**$kv_{app}{}^{\beta \to \alpha}$ (min^{-1})**	
Column Temp. (K)	**Auto-DHPLC-Y2K**	**DCXplorer**	**Auto-DHPLC-Y2K**	**DCXplorer**	**Auto-DHPLC-Y2K**	**DCXplorer**	**Auto-DHPLC-Y2K**	**DCXplorer**
298.15	21.774	21.799	0.4080×10^{-1}	0.3816×10^{-1}	22.211	22.165	0.1951×10^{-1}	0.2058×10^{-1}
288.15	21.376	21.484	0.2373×10^{-1}	0.2282×10^{-1}	21.875	21.838	0.1164×10^{-1}	0.1322×10^{-1}
278.15	21.056	21.063	0.9931×10^{-2}	0.9534×10^{-2}	21.451	21.401	0.4862×10^{-2}	0.5148×10^{-2}

Table 3. Values of $\Delta G^{\#}$ and kv_{app} for the processes that lead from the α to the β anomer of D-Xylose, and vice-versa, obtained by simulating experimental dynamic chromatograms with the Auto-DHPLC-Y2K and DCXplorer programs.

	D-Xylose							
	$\alpha \to \beta$				**$\beta \to \alpha$**			
	$\Delta G^{\#}{}_{\alpha \to \beta}$ (kcal mol^{-1})		**$kv_{app}{}^{\alpha \to \beta}$ (min^{-1})**		**$\Delta G^{\#}{}_{\beta \to \alpha}$ (kcal mol^{-1})**		**$kv_{app}{}^{\beta \to \alpha}$ (min^{-1})**	
Column Temp. (K)	**Auto-DHPLC-Y2K**	**DCXplorer**	**Auto-DHPLC-Y2K**	**DCXplorer**	**Auto-DHPLC-Y2K**	**DCXplorer**	**Auto-DHPLC-Y2K**	**DCXplorer**
298.15	21.213	21.360	0.1051	0.0801×10^{-1}	21.542	21.596	0.6030×10^{-1}	0.5367×10^{-1}
288.15	20.906	21.124	0.5179×10^{-1}	0.4243×10^{-1}	21.298	21.353	0.2985×10^{-1}	0.2739×10^{-1}
278.15	20.717	20.854	0.1830×10^{-1}	0.1398×10^{-1}	21.031	21.073	0.1038×10^{-1}	0.0936×10^{-1}

3.4. Dynamic HILIC for Interconverting α/β Anomers

Interconversion of α/β anomers of monosaccharides (anomerization) is a particular case of isomerization process that can be conveniently studied by the use of the D-HILIC. In this work, the anomerization of D-glucose and D-xylose has been investigated. The

relevant dynamic chromatograms (obtained in the range of temperatures from 5 to 50 °C using VSG_HD-1-Photo-Cys and acetonitrile/water 85/15% *v/v* as mobile phase) have been reported in Figure 3. Experimental chromatographic profiles (in red) are well super-imposable to the simulated ones (in blue) both in the plateau region as well at the start or the end of elution peak thanks also to the good symmetry of peaks, making this media a good candidate for dynamic studies by using Auto-DHPLC-Y2K.
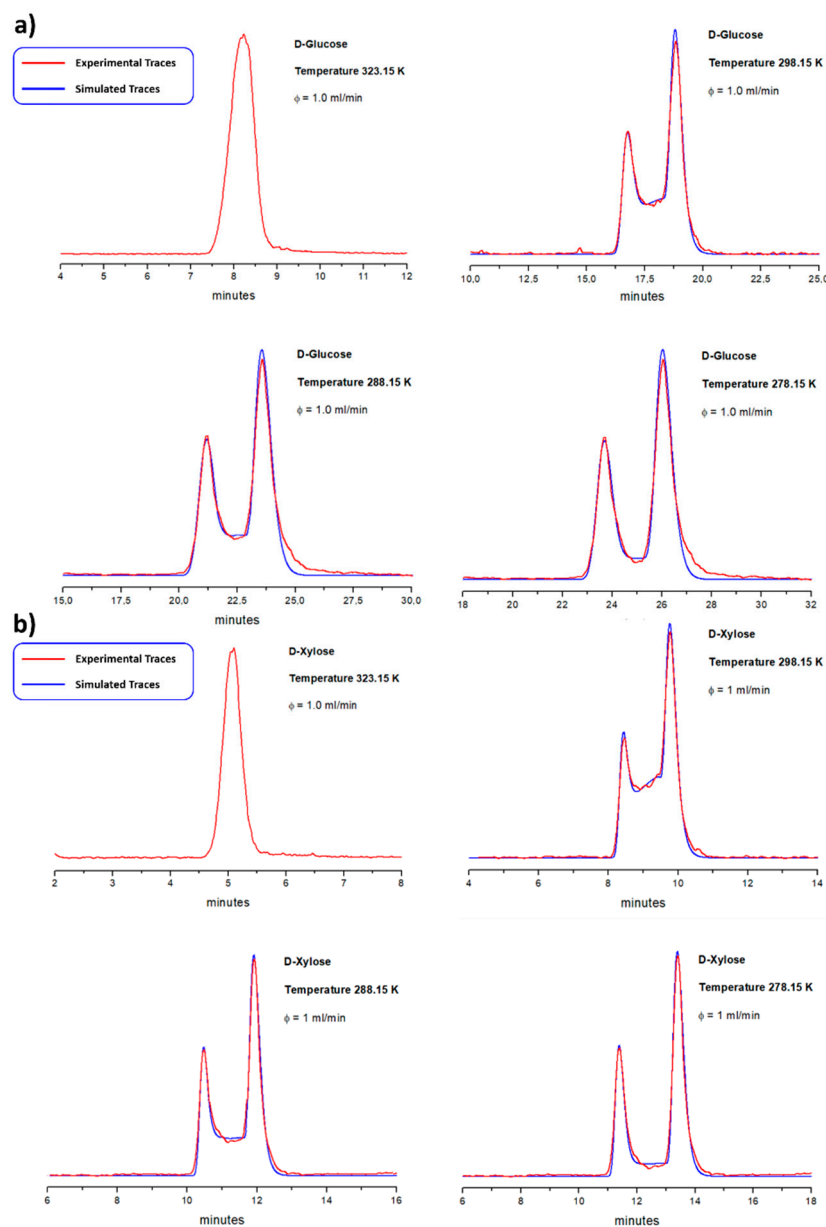

Figure 3. Experimental dynamic chromatograms of (**a**) D-glucose and (**b**) D-xylose registered at different temperatures (red traces) and their superimposed simulations (blue traces), performed with the Auto-DHPLC-Y2K software. Experimental conditions: cysteine stationary phase column (5 μm, 150 × 4.6 mm L × I.D.). mobile phase: acetonitrile/water 85/15 (% *v/v*), flow rate: 1.0 mL/min; detector: ELSD (T_{Drift}: 70 °C; P: 45 psi; Gain: 10).

The relative percentages of α and β anomers, at equilibrium, were determined by ^{1}H-NMR analysis (Figure 4) in the deuterated solvent mixture corresponding to the mobile phase (CD_3CN/D_2O in a ratio of 85/15% *v/v*). This necessary information was subsequently employed in performing the simulation of the dynamic chromatograms visible as blue traces in Figure 3.

Figure 4. ^{1}H-NMR spectra (CD$_3$CN/D$_2$O 85/15% *v/v*) of a solution of D-glucose [2 mg/mL] and of a solution of D-xylose [2 mg/mL] both equilibrated at 25 °C for 72 h in order to determine the anomeric ratio α/β.

By integration of ^{1}H-NMR signals (Figure 4), the following α/β rations were found: (i) D-glucose, α/β = 35/65; (ii) D-xylose, α/β = 40/60. These results are consistent with relevant literature data obtained using ^{1}H-NMR technique and other types of analytical approaches [16,33–39]. Chromatographic analyses of D-glucose and D-xylose, conducted with the VSG_HD-1-Photo-Cys at 5 °C, 15 °C and 25 °C, revealed efficient resolutions of α and β anomers, but also active interconversion between them, as evidenced by the presence of plateau zones between the two well-separated peaks. These dynamic chromatograms, reported in Figure 3, show the type II morphology, therefore are suitable for computational simulation for extracting kinetic data of the anomerization phenomenon. Instead, coalescence of the peaks is observed at the temperature of 50 °C, giving rise to a dynamic chromatogram of morphology corresponding to that reported as case I in Figure 3, it is not suitable to extract reliable kinetic information from computational simulation. Inspection of kinetic data reported in Table 2 highlights for D-xylose a bit faster anomerization compared with D-glucose. Thus, at room temperature, the activation barriers (calculated as average of the values resulting by simulations with both Auto-DHPLC-Y2K and DCXplorer softwares) differ by 0.5 kcal/mol for the α→β isomerization (from $^{Glu}\Delta G^{\#}_{\alpha\to\beta}$ = 21.8 kcal/mol to $^{Xyl}\Delta G^{\#}_{\alpha\to\beta}$ = 21.3 kcal/mol) and by 0.6 kcal/mol for the backward β→α process (from $^{Glu}\Delta G^{\#}_{\beta\to\alpha}$ = 22.2 kcal/mol to $^{Xyl}\Delta G^{\#}_{\beta\to\alpha}$ = 21.6 kcal/mol).

The Gibbs activation energy variations are consistent with the data reported in the literature, both performed by computational calculations at B3PW91/6-31G (d, p) level [40], and by experimental approach, among which the D-HILIC technique [16].

The relevant activation free energy barriers ($\Delta G^{\#}_{a\to b}$ and $\Delta G^{\#}_{a\leftarrow b}$) can be obtained by use of the Eyring-Polanyi Equation (1):

$$\Delta G^{\#}(T) = -RT\ln\left(\frac{k_1 h}{k_b T_k}\right) \tag{1}$$

In Equation (1) k_B is the Boltzmann constant ($k_B = 1.380649 \times 10^{-23}$ J K^{-1}), R the gas constant (R = 8.31441 J K^{-1} mol^{-1}), T the isomerization temperature (in K), h the Planck's constant (h = 6.62617×10^{-34} J s^{-1}) and k_1 the reaction rate constant.

If the kinetic study is repeated at different temperatures, the related enthalpic and entropic contributions of $\Delta G^{\#}$ (i.e., $\Delta H^{\#}$ and $\Delta S^{\#}$) are also determinable, as slope and intercept of van't Hoff plots in which $\Delta G^{\#}/T$ is reported versus $1/T$, as suggested by the Gibbs equation rewritten in the form shown below:

$$\frac{\Delta G^{\#}}{T} = \frac{\Delta H^{\#}}{T} - \Delta S^{\#} \tag{2}$$

As previously stated, the dynamic chromatograms were registered at three different temperatures. The kinetic data, obtained from their suitable simulation through both the computational programs Auto-DHPLC-Y2K and DCXplorer, have next been converted into the related $\Delta G^{\#}$ values by means of Equation (1). Finally, by van't Hoff analyses (i.e., realization of the $\Delta G^{\#}/T$ vs. $1/T$ plots reported in Figure 5), these activation thermodynamic data have been employed to extrapolate the relevant $\Delta H^{\#}$ and $\Delta S^{\#}$ contributions of the studied interconversion processes.
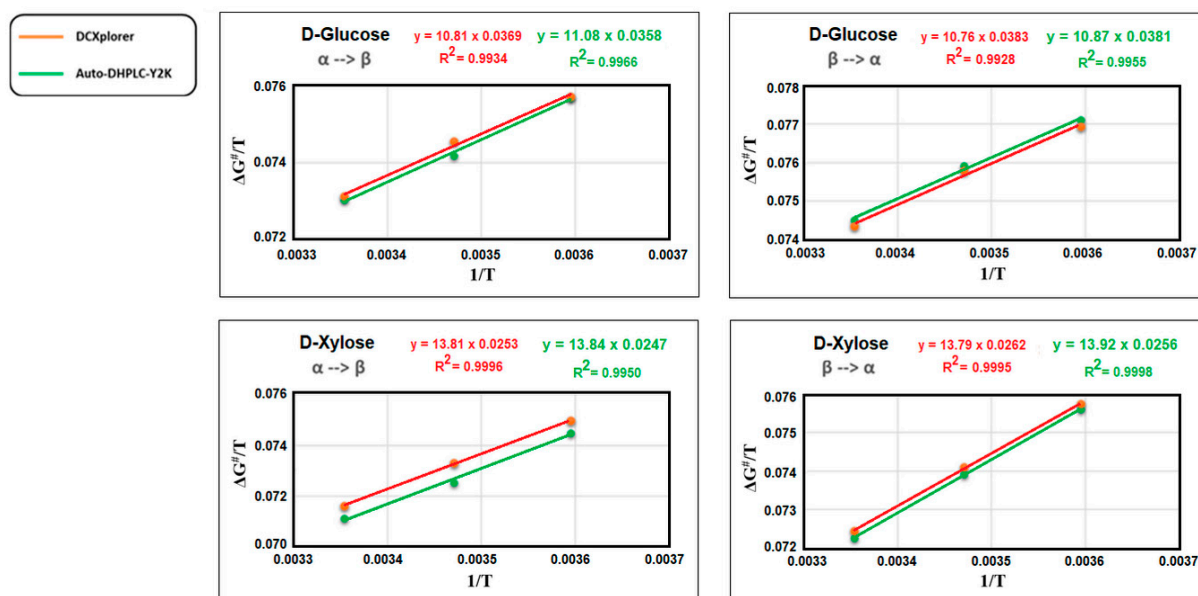

Figure 5. Comparison of the van't Hoff plots obtained by using $\Delta G^{\#}$ values computed from the related kv_{app} data evaluated through the simulations of computational programs Auto-DHPLC-Y2K, green line, and DCXplorer, red line.

From inspection of the $\Delta G^{\#}/T$ vs. $1/T$ plots of Figure 5 the obtaining of excellent linear correlations, with R^2 never lesser than 0.9928, is evident, as well as it is also clear the reliability of the obtained values of $\Delta H^{\#}$ and $\Delta S^{\#}$, highlighted by the good convergence of results gained with the two independent programs used in the analyses of dynamic chromatograms (data reported in Table 4).

Table 4. Values of $\Delta S^{\#}$ (e.u.) and of $\Delta H^{\#}$ (kcal mol^{-1}) of the interconversion reactions under examination of D-Glucose and D-Xylose, obtained through van't Hoff analysis.

	D-Glucose				D-Xylose			
	$\alpha\rightarrow\beta$		$\beta\rightarrow\alpha$		$\alpha\rightarrow\beta$		$\beta\rightarrow\alpha$	
	Auto DHPLC Y2K	DCXplorer	Auto DHPLC Y2K	DCXplorer	Auto DHPLC Y2K	DCXplorer	Auto DHPLC Y2K	DCXplorer
$\Delta S^{\#}$ (e.u.)	−35.8	−36.9	−38.10	−38.30	−24.70	−25.30	−25.60	−26.20
$\Delta H^{\#}$ (kcal mol^{-1})	11.08	10.81	10.87	10.76	13.84	13.81	13.92	13.79

4. Conclusions

A new HPLC column packed with immobilized cysteine by a photo-click procedure (i.e., VSG_HD-1-Photo-Cys) was prepared and evaluated for its carbohydrate isomer separation capability under hydrophilic interaction liquid chromatography (HILIC) conditions with evaporative light scattering detection.

Both D-glucose and D-Xylose were analysed using the VSG_HD-1-Photo-Cys column, and the resulting chromatograms registered at the temperature of 5, 15, and 25 °C showed a dynamically deformed HPLC plot featuring a plateau zone between the resolved peaks, with the size and shape of the plateau zone dependent on anomerization rate and α/β equilibrium composition. Rate constants for the forward ($\alpha\rightarrow\beta$) and backward ($\beta\rightarrow\alpha$) anomerization (and therefore from them also the corresponding energy barriers by means of the Eyring-Polanyi equation) were calculated by suitable simulation of the dynamic chromatograms performed with dedicated programs. In the whole, for glucose, in the temperature interval from 5 to 25 °C, the detected anomerization energy barriers range from 22.2 to 21.1 kcal/mol and the difference between forward ($\alpha\rightarrow\beta$) and backward ($\beta\rightarrow\alpha$) reaction is around 0.40 kcal/mol (averaged value). For xylose, always in the temperature interval from 5 to 25 °C, the found anomerization energy barriers fall overall within the range from 21.6 to 20.7 kcal/mol, and the observed difference between forward ($\alpha\rightarrow\beta$) and backward ($\beta\rightarrow\alpha$) reaction is around 0.29 kcal/mol (averaged value).

Author Contributions: Conceptualization, S.M., M.P. and C.V.; methodology, S.M.; software, M.P.; validation, A.C. and A.F.; formal analysis, F.B. and A.C.; investigation, F.B. and A.F.; resources, M.P.; data curation, S.M. and F.B.; writing—original draft preparation, F.B. and S.M.; writing—review and editing, S.M. and M.P.; visualization, C.V. and M.P.; supervision, C.V.; funding acquisition, M.P. All authors have read and agreed to the published version of the manuscript.

Conflicts of Interest: The authors declare no conflict of interest.

References

1. Yan, J.; Shi, S.; Wang, H.; Liu, R.; Li, N.; Chen, Y.; Wang, S. Neutral monosaccharide composition analysis of plant-derived oligo- and polysaccharides by high performance liquid chromatography. *Carbohydr. Polym.* **2016**, *136*, 1273–1280. [CrossRef] [PubMed]
2. Afshari, K.; Samavati, V.; Shahidi, S.-A. Ultrasonic-assisted extraction and in-vitro antioxidant activity of polysaccharide from Hibiscus leaf. *Int. J. Biol. Macromol.* **2015**, *74*, 558–567. [CrossRef] [PubMed]

3. Courtois, J. Oligosaccharides from land plants and algae: Production and applications in therapeutics and biotechnology. *Curr. Opin. Microbiol.* **2009**, *12*, 261–273. [CrossRef] [PubMed]

4. Pazourek, J. Monitoring of mutarotation of monosaccharides by hydrophilic interaction chromatography. *J. Sep. Sci.* **2010**, *33*, 974–981. [CrossRef]

5. El Khadem, H. (Ed.) *Carbohydrate Chemistry: Monosaccharides and Their Oligomers*; Elsevier: Amsterdam, The Netherlands, 2012.

6. Ikegami, T.; Horie, K.; Saad, N.; Hosoya, K.; Fiehn, O.; Tanaka, N. Highly efficient analysis of underivatized carbohydrates using monolithic-silica-based capillary hydrophilic interaction (HILIC) HPLC. *Anal. Bioanal. Chem.* **2008**, *391*, 2533–2542. [CrossRef]

7. Li, S.P.; Wu, D.T.; Lv, G.P.; Zhao, J. Carbohydrates analysis in herbal glycomics. *TrAC Trends Anal. Chem.* **2013**, *52*, 155–169. [CrossRef]

8. Dai, J.; Wu, Y.; Chen, S.-W.; Zhu, S.; Yin, H.-P.; Wang, M.; Tang, J. Sugar compositional determination of polysaccharides from Dunaliella salina by modified RP-HPLC method of precolumn derivatization with. *Carbohydr. Polym.* **2010**, *82*, 629–635. [CrossRef]

9. Jandera, P.; Janás, P. Recent advances in stationary phases and understanding of retention in hydrophilic interaction chromatography. A review. *Anal. Chim. Acta* **2017**, *967*, 12–32. [CrossRef]

10. Zhang, S.; Li, C.; Zhou, G.; Che, G.; You, J.; Suo, Y. Determination of the carbohydrates from Notopterygium forbesii Boiss by HPLC with fluorescence detection. *Carbohydr. Polym.* **2013**, *97*, 794–799. [CrossRef]

11. Bean, S.R.; Ioerger, B.P.; Blackwell, D.L. Separation of kafirins on surface porous reversed-phase high-performance liquid chromatography columns. *J. Agric. Food Chem.* **2011**, *59*, 85–91. [CrossRef]

12. Jandera, P. Stationary and mobile phases in hydrophilic interaction chromatography: A review. *Anal. Chim. Acta* **2011**, *692*, 1–25. [CrossRef] [PubMed]

13. Martín-Ortiz, A.; Carrero-Carralero, C.; Hernández-Hernández, O.; Lebrón-Aguilar, R.; Moreno, F.; Sanz, M.; Ruiz-Matute, A. Advances in structure elucidation of low molecular weight carbohydrates by liquid chromatography-multiple-stage mass spectrometry analysis. *J. Chromatogr. A* **2019**, *1612*, 460664. [CrossRef] [PubMed]

14. Montesano, D.; Cossignani, L.; Giua, L.; Urbani, E.; Simonetti, M.S.; Blasi, F. A Simple HPLC-ELSD Method for Sugar Analysis in Goji Berry. *J. Chem.* **2016**, *2016*, 1–5. [CrossRef]

15. Soyseven, M.; Sezgin, B.; Arli, G. A novel, rapid and robust HPLC-ELSD method for simultaneous determination of fructose, glucose and sucrose in various food samples: Method development and validation. *J. Food Compos. Anal.* **2022**, *107*, 104400. [CrossRef]

16. Fu, X.; Cebo, M.; Ikegami, T.; Lämmerhofer, M. Separation of carbohydrate isomers and anomers on poly-N-(1H-tetrazole-5-yl)-methacrylamide-bonded stationary phase by hydrophilic interaction chromatography as well as determination of anomer interconversion energy barriers. *J. Chromatogr. A* **2020**, *1620*, 460981. [CrossRef]

17. Bennett, R.; Olesik, S.V. Gradient separation of oligosaccharides and suppressing anomeric mutarotation with enhanced-fluidity liquid hydrophilic interaction chromatography. *Anal. Chim. Acta* **2017**, *960*, 151–159. [CrossRef]

18. Kouzounis, D.; Sun, P.; Bakx, E.J.; Schols, H.A.; Kabel, M.A. Strategy to identify reduced arabinoxylo-oligosaccharides by HILIC-MSn. *Carbohydr. Polym.* **2022**, *289*, 119415. [CrossRef]

19. Moni, L.; Ciogli, A.; D'Acquarica, I.; Dondoni, A.; Gasparrini, F.; Marra, A. Synthesis of Sugar-Based Silica Gels by Copper-Catalysed Azide-Alkyne Cycloaddition via a Single-Step Azido-Activated Silica Intermediate and the Use of the Gels in Hydrophilic Interaction Chromatography. *Chem.-A Eur. J.* **2010**, *16*, 5712–5722. [CrossRef]

20. Pazourek, J. Determination of glucosamine and monitoring of its mutarotation by hydrophilic interaction liquid chromatography with evaporative light scattering detector. *Biomed. Chromatogr.* **2018**, *32*, e4368. [CrossRef]

21. Galant, A.L.; Kaufman, R.C.; Wilson, J.D. Glucose: Detection and analysis. *Food Chem.* **2015**, *188*, 149–160. [CrossRef]

22. Lopes, E.; Gaspar, J.F. Simultaneous chromatographic separation of enantiomers, anomers and structural isomers of some biologically relevant monosaccharides. *J. Chromatogr. A* **2008**, *1188*, 34–42. [CrossRef] [PubMed]

23. Gangola, M.P.; Jaiswal, S.; Khedikar, Y.P.; Chibbar, R.N. A reliable and rapid method for soluble sugars and RFO analysis in chickpea using HPAEC–PAD and its comparison with HPLC–RI. *Food Chem.* **2014**, *154*, 127–133. [CrossRef] [PubMed]

24. Rohrer, J.S.; Basumallick, L.; Hurum, D. High-performance anion-exchange chromatography with pulsed amperometric detection for carbohydrate analysis of glycoproteins. *Biochemistry* **2013**, *78*, 697–709. [CrossRef] [PubMed]

25. Ortner, F.; Wiemeyer, H.; Mazzotti, M. Interconversion and chromatographic separation of carbohydrate stereoisomers on polystyrene-divinylbenzene resins. *J. Chromatogr. A* **2017**, *1517*, 54–65. [CrossRef]

26. Gasparrini, F.; D'Acquarica, I.; Pierini, M.; Villani, C.; Ismail, O.H.; Ciogli, A.; Cavazzini, A. *Chapter 3—Chiral Separations. Chiral Dynamic Chromatography in the Study of Stereolabile Compounds*; Elsevier: Amsterdam, The Netherlands, 2017. [CrossRef]

27. Cabri, W.; Ciogli, A.; Dacquarica, I.; DiMattia, M.; Galletti, B.; Gasparrini, F.; Giorgi, F.; Lalli, S.; Pierini, M.; Simone, P. On-column epimerization of dihydroartemisinin: An effective analytical approach to overcome the shortcomings of the International Pharmacopoeia monograph. *J. Chromatogr. B Anal. Technol. Biomed. Life Sci.* **2008**, *875*, 180–191. [CrossRef] [PubMed]

28. Trapp, O.; Schurig, V. ChromWin—A computer program for the determination of enantiomerization barriers in dynamic chromatography. *Comput. Chem.* **2001**, *25*, 187–195. [CrossRef]

29. Trapp, O. A novel software tool for high throughput measurements of interconversion barriers: DCXplorer. *J. Chromatogr. B Anal. Technol. Biomed. Life Sci.* **2008**, *875*, 42–47. [CrossRef] [PubMed]

30. Ciogli, A.; Buonsenso, F.; Proietti, N.; Mazzoccanti, G.; Manetto, S.; Calcaterra, A.; De Angelis, M.; Gasparrini, F. Preparation of a high-density vinyl silica gel to anchor cysteine via photo-click reaction and its applications in hydrophilic interaction chromatography. *J. Chromatogr. A* **2022**, *1675*, 463173. [CrossRef]

31. Shen, A.; Guo, Z.; Yu, L.; Cao, L.; Liang, X. A novel zwitterionic HILIC stationary phase based on "thiol-ene" click chemistry between cysteine and vinyl silica. *Chem. Commun.* **2011**, *47*, 4550–4552. [CrossRef]

32. Mojsiewicz-Pieńkowska, K. On the Issue of Characteristic Evaporative Light Scattering Detector Response. *Crit. Rev. Anal. Chem.* **2009**, *39*, 89–94. [CrossRef]

33. Bubb, W.A. NMR spectroscopy in the study of carbohydrates: Characterizing the structural complexity. *Concepts Magn. Reson. Part A Bridg. Educ. Res.* **2003**, *19*, 1–19. [CrossRef]

34. Lemieux, J.D.; Stevens, R.U. The Proton Magnetic Resonance Spectra and Tautomeric Equilibria of Aldoses in Deuterium Oxide. *Can. J. Chem.* **1966**, *44*, 249–262. [CrossRef]

35. Angyal, S.J. The Composition of Reducing Sugars in Solution: Current Aspects. *Adv. Carbohydr. Chem. Biochem.* **1991**, *49*, 19–35. [CrossRef]

36. Le Barc'H, N.; Grossel, J.M.; Looten, P.; Mathlouthi, M. Kinetic study of the mutarotation of D-glucose in concentrated aqueous solution by gas-liquid chromatography. *Food Chem.* **2001**, *74*, 119–124. [CrossRef]

37. Kabayama, M.A.; Patterson, D. The thermodynamics of mutarotation of some sugars: II. Theoretical considerations. *Can. J. Chem.* **1958**, *36*, 563–573. [CrossRef]

38. Hoog, C.; Widmalm, G. Free Energy Simulations of D-Xylose in Water and Methyl D-Xylopyranoside in Methanol Christer. *J. Phys. Chem. B* **2001**, *105*, 6375–6379. [CrossRef]

39. Drew, K.N.; Zajicek, J.; Bondo, G.; Bose, B.; Serianni, A.S. 13C-labeled aldopentoses: Detection and quantitation of cyclic and acyclic forms by heteronuclear 1D and 2D NMR spectroscopy. *Carbohydr. Res.* **1998**, *307*, 199–209. [CrossRef]

40. Lewis, B.E.; Choytun, N.; Schramm, V.L.; Bennet, A.J. Transition States for Glucopyranose Interconversion. *J. Am. Chem. Soc.* **2006**, *128*, 5049–5058. [CrossRef]